phys. stat. sol. (b) **215**, 1067 (1999)

Subject classification: 72.20.Fr; 72.20.Dp; 75.50.Pp; S8.16

Electrical Properties of the $Cu_2FeGeSe_4$ Compound

G. SÁNCHEZ PORRAS, M. QUINTERO, R. BARRIOS, J. GONZALEZ, R. TOVAR, and J. RUIZ

Centro de Estudios de Semiconductores, Departamento de Física, Facultad de Ciencias, Universidad de Los Andes, Mérida 5101, Venezuela

(Received December 28, 1998; in revised form May 26, 1999)

The electrical transport properties of a polycrystalline sample of $Cu_2FeGeSe_4$ magnetic semiconductor compound are studied in the temperature range between 100 and 300 K. From the analysis of the electrical data, the values of the activation energy E_A, the density of states effective mass of the holes m_p, the concentration of the ionized impurities N_I, the sound velocity v and the valence-band deformation potential E_{ac} for the compound are estimated.

1. Introduction

Magnetic semiconducting materials are of interest because of the manner in which the magnetic behavior associated with the concerned magnetic ion can modify and complement the semiconductor properties [1, 2]. The materials that have been mostly studied are the semimagnetic semiconductor alloys obtained from the tetrahedrally coordinated II–VI semiconductor compounds by replacing a fraction of the group II cations with manganese, giving alloys which show spin-glass behavior, very large magneto-optical effects, etc. [1, 2]. It was recently suggested [3, 4] that another set of magnetic compounds and alloys, which could show larger magneto-optical effect than the II–VI derived alloys, can be obtained from the tetrahedral bonded I_2–II–IV–VI_4 compounds by replacing the II cations with Mn, Fe, Co and/or Ni ions. $Cu_2FeGeSe_4$ belongs to this family of compounds. The crystallographic properties of these materials have been studied by several workers [5, 6], and it has been found that the $Cu_2FeGeSe_4$ compound has the stannite tetragonal structure ($I\bar{4}2m$) with lattice parameters $a = 5.5096$ Å and $c = 11.030$ Å [5]. Analysis of the magnetic susceptibility as a function of temperature showed that $Cu_2FeGeSe_4$ is antiferromagnetic with a Néel temperature $T_N = 20.0$ K and a Curie-Weiss temperature $\theta_a = -155.05$ K. Also, from analysis of the electrical resistivity, susceptibility and magnetization results [5], the presence of bound magnetic polarons (BMPs) in this sample was found, which were associated with a shallow acceptor level in agreement with earlier studies made on this type of materials [1, 2].

The study of the electrical transport properties, which would give useful information about the impurity levels and the band parameters for $Cu_2FeGeSe_4$, has not been reported. Hence, in this paper, the temperature dependence of the resistivity, charge carrier concentration and mobility between 100 and 300 K are studied. From the analysis, an attempt is made to determine the acceptor ionization energy, the density of states effective mass of holes, the valence-band deformation potential and the sound velocity of this compound.

2. Sample Preparation and Experimental Measurements

The sample used was prepared by the melt and anneal technique, the description of the preparation of this material having been published previously [6]. The equilibrium condition of the prepared sample was determined from Guinier X-ray powder photographs. It was found that an annealing period from twenty to thirty days produces a sample in good equilibrium conditions with the stannite structure, and no traces of secondary phases were observed in the X-ray pattern.

A small slice of about 0.5 mm thickness was cut from the ingot for the electrical measurements. The conductivity of the sample, as checked by a thermal probe, was found to be p-type. Electrical contacts to the sample were made by electroplating four symmetrical copper spots, which were used as a basis for soldering copper leads with indium. These contacts were ohmic in nature through all the temperature range of the present measurements. The electrical conductivity and the Hall mobility μ_H in a magnetic field of 10 kOe were measured by the van der Pauw method. The error in the carrier concentration and mobility measurements was estimated to be about $\pm 5\%$.

3. Experimental Results and Discussion

3.1 Resistivity and hole concentration

The resistivity ϱ was measured in the temperature range from 100 to 300 K and the resulting log (ϱ) versus. $1000/T$ curve is shown in Figure 1a. It is seen that, within the limits of experimental error, this variation appears to be nearly linear and that ϱ increases as T is decreased. The hole binding energy E_A was estimated from the slope of the log (ϱ) versus $1000/T$ curve, and the resulting value was found to be $E_A \approx 42$ meV, with an uncertainty of about 10%. As was indicated in a previous work [6], these shallow acceptor levels favor the presence of BMPs in this sample. The magnetic results obtained for this sample together with a quantitative analysis made on BMPs will be presented in a further work.

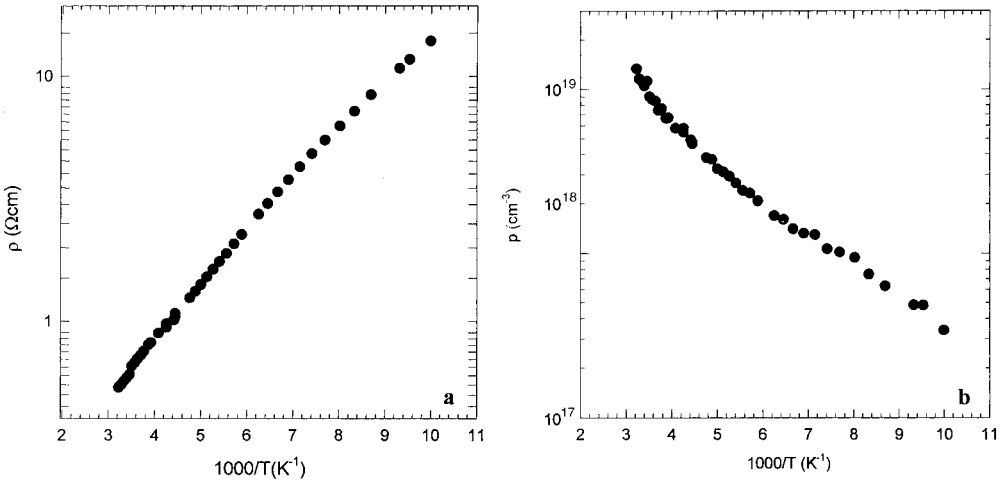

Fig. 1. Variation of a) resistivity ϱ and b) hole concentration p with T for $Cu_2FeGeSe_4$

The hole concentration p, plotted as a function of temperature between 100 and 300 K for the $Cu_2FeGeSe_4$ compound, is shown in Fig. 1b. It is observed that p increases with the increase of the temperature. This behavior of p and that of the resistivity ϱ shown in Fig. 1a are typical for a semiconductor material.

To get an estimate of the activation energy E_A of the acceptor level and the density of states effective mass m_p, the temperature dependence of the hole concentration was analyzed using the following expression for the nondegenerate statistics of a single level [7]:

$$\frac{p(p+N_d)}{(N_a-N_d-p)}=\frac{2(2\pi m_p kT/h^2)^{3/2}}{\beta}\exp(-E_A/kT), \tag{1}$$

where N_a and N_d are the acceptor and compensating donor densities, respectively, and β is the impurity degeneracy, which is taken to be two in the present case. It is also assumed that N_a, N_d, E_A and m_p are parameters independent of temperature.

The criteria used to determine these parameters were to choose values of N_a and N_d until a linear plot of

$$\ln[p(p+N_d)/(N_a-N_d-p)T^{3/2}] \text{ versus } 1000/T, \tag{2}$$

including the maximum numbers of experimental points was obtained. Then a linear least-squares fit to these points was carried out. The resulting fit, thus obtained, is shown in Fig. 2. The activation energy E_A estimated from the slope of that line was found to be (43.4 ± 1.4) meV. This value is very close to the one estimated from the resistivity data in Fig. 1a. The resulting values of N_a and N_d were $2\times10^{19}\,cm^{-3}$ and $1\times10^{18}\,cm^{-3}$, respectively. The density of states effective mass m_p value determined from the intercept at $T\to\infty$ was found to be $1.32m_0$. This value is similar to those given in the literature for $CuGaSe_2$ ($m_p/m_0=1.20$), $CuInS_2$ ($m_p/m_0=1.30$) and $CuGaTe_2$ ($m_p/m_0=1.30$) tetragonal chalcopyrite compounds [8, 9]. These parameters are given in Table 1.

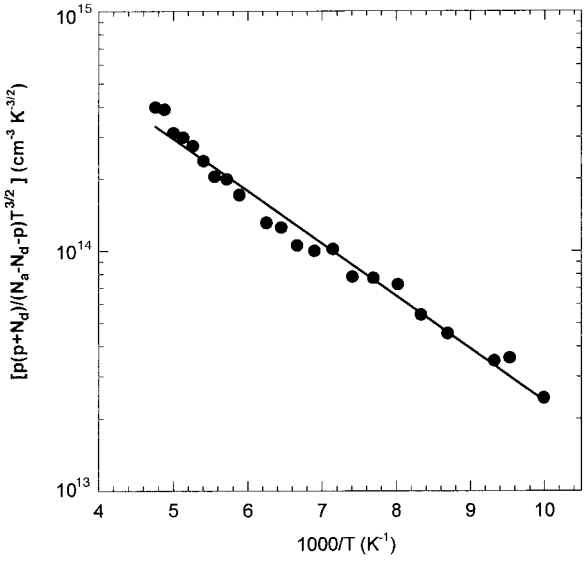

Fig. 2. Plot of $\ln[p(p+N_d)/(N_a-N_d-p)T^{3/2}]$ vs. $10^3/T$ for $Cu_2FeGeSe_4$

Table 1

Value of ϱ_0 calculated from the lattice constants quoted above. Values of N_a, N_d, $N_I = N_d + N_a$, E_A and m_p/m_0 estimated from eq. (1). The final values of parameters ε, v, E_{ac} and B obtained from fitting the mobility data using $\mu^{-1} = \mu_I^{-1} + \mu_{acnpo}^{-1} + \mu_{sc}^{-1}$, with $\theta = 500$ K, $\eta = 4$, $H = 1.34$ and $D = 0.914$ from Ref. [10]

ϱ_0 (g/cm^3)	N_d (cm^{-3})	N_a (cm^{-3})	E_A (meV)	m_p/m_0
5.50	2×10^{19}	1×10^{18}	43.4 ± 1.4	1.32
ε	v (10^5 cm/s)	E_{ac}*)	N_I (cm^{-3})	B (cm^{-3})
2.7 ± 0.2	1.9 ± 0.1	16 ± 0.5	2.1×10^{19}	512 ± 65

*) E_{ac} in eV/unit dilation.

3.2 Hole mobility

The Hall mobility μ_H for the compound is plotted as a function of temperature T between 100 and 300 K in Fig. 3. It is seen that the variation of μ_H with T is very small. However, an attempt to analyze the data will be made here. Hence, to explain the μ versus T results, the scattering of the charge carriers by ionized impurities, the combined acoustic and nonpolar optical mode effects as well as the space-charge contribution have to be taken into account. Based on the work of Wiley and DiDomenico [10] in the present analysis of a p-type sample, the contribution due to polar optical modes is not considered.

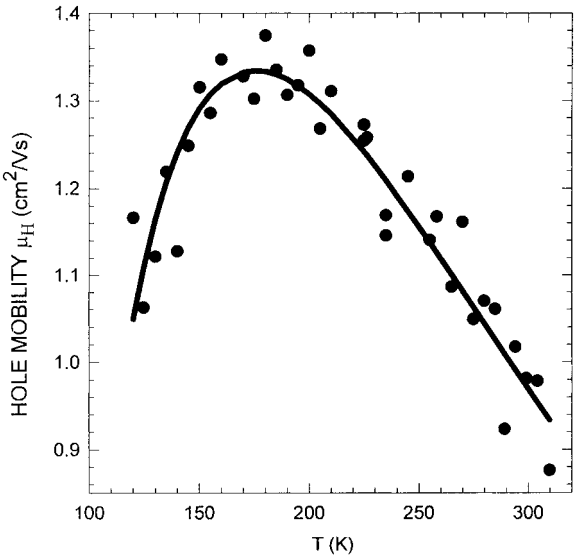

Fig. 3. Variation of the hole mobility with T for $Cu_2FeGeSe_4$. Full circles: experimental data, full curve: fitted to $\mu^{-1} = \mu_I^{-1} + \mu_{acnpo}^{-1} + \mu_{sc}^{-1}$

The Hall mobility due to ionized impurities is given, according to the Brooks-Herring relation [11], by

$$\mu_{\mathrm{I}} = \left(\frac{2}{300}\right) \frac{2^{7/2}\varepsilon^2 (kT)^{3/2}}{\pi^{3/2} e^3 (m_{\mathrm{p}})^{1/2} N_{\mathrm{I}} f(x)} \quad [\mathrm{cm^2\ V^{-1}\ s^{-1}}] \tag{3}$$

where N_{I} is the density of ionized impurities, e is the elementary electronic charge and ε is the low frequency dielectric constant. The function $f(x)$ is given by $\ln(1+x) - x/(1+x)$, where

$$x = [6\varepsilon m_{\mathrm{p}} (kT)^2]/(\pi e^2 \hbar^2 p)\,. \tag{4}$$

The combined effect of the acoustic and nonpolar optical mode scattering is given by the expression [10]

$$\mu_{\mathrm{acnpo}} = \mu_{\mathrm{ac}} S(\theta, \eta, T)\,. \tag{5}$$

Here, θ is the optical phonon characteristic temperature and $\eta \approx (E_{\mathrm{acnpo}}/E_{\mathrm{ac}})^2$, where E_{acnpo} and E_{ac} are the nonpolar optical and acoustic mode deformation potentials, respectively. An analytical approximation to $S(\theta, \eta, T)$ is found to be [10]

$$S(\theta, \eta, T) \cong (1 + A\eta)^{-1}\,, \tag{6}$$

with

$$A = Hz/(e^z - D)\,, \tag{7}$$

where the constants H and D have been tabulated for each value of η [10] and $z = \theta/T$.

For the acoustic mode scattering mobility, the expression [12] used is

$$\mu_{\mathrm{ac}} = \left(\frac{2}{300}\right) \frac{(8\pi)^{1/2} e \hbar^4 \varrho_0 v^2}{3E_{\mathrm{ac}}^2 (m_{\mathrm{p}})^{5/2} (kT)^{3/2}} \quad [\mathrm{cm^2\ V^{-1}\ s^{-1}}]\,, \tag{8}$$

where ϱ_0 is the mass density and v the sound velocity in the material.

For the space-charge scattering contribution to the mobility, assuming, to a first approximation, that the current carriers cannot penetrate into the space-charge centers and then treats the scattering as a simple collision problem, then the space-charge scattering contribution to the mobility for both spherical and cylindrical space centers is given by [15]

$$\mu_{\mathrm{sc}} = (2/300)\, B (p/p_{300})^{1/3}\, (T/300)^{-5/6}\, [\mathrm{cm^2/V\ s}]\,, \tag{9}$$

where B is a constant given by

$$B = (N_{\mathrm{S}}\sigma)^{-1}\,.$$

Here N_{S} is the density of space-charge centers and σ is their effective scattering cross-section, p is the hole concentration, which in the present case is given in Fig. 1b, and p_{300} is the hole concentration at 300 K.

To calculate the total mobility, Mathiessen's approximation [13] $\mu^{-1} = \Sigma \mu_i^{-1}$ has been used. To carry out a theoretical fit to the mobility data, information about several material parameters such as ϱ_0, m_{p}/m_0, ε, v, E_{ac} and N_{I} is required. From the lattice parameter constants, quoted above, the value of ϱ_0 has been calculated to be 5.50 g/cm^3.

The value of $m_p = 1.32m_0$ has been estimated from Fig. 2. The mobility data were fitted using the standard nonlinear least-squares Levenberg-Marquardt method [14] to determine the parameters that minimize the sum of squares of differences between the dependent variable values in the theoretical equation and the experimental data. Then, the criterion of the minimum standard deviations was used to select these parameters. In the initial analysis, equations (3) to (8), with ε, v, E_{ac} and N_I treated as adjustable parameters, were used to fit the experimental data. It was found that a good fit could be obtained without taking into account the scattering term due to the space-charge contribution giving parameters values of $\varepsilon = 10$, $v = 2.0 \times 10^5$ cm/s, $E_{ac} = 15.9$ eV/unit dilation and $N_I = 2.2 \times 10^{20}\,\mathrm{cm}^{-3}$. The value of $N_I = 2.2 \times 10^{20}$ cm^{-3} so obtained is much larger than the value $N_d + N_a = 2.1 \times 10^{19}$ cm^{-3} obtained from Fig. 2. However, it was found that when including also the space-charge term, eq. (9), and using the value of $N_I = 2.1 \times 10^{19}\,\mathrm{cm}^{-3}$ determined from Fig. 2 and taking $\theta = 500$ K, $\eta = 4$, $H = 1.34$ and $D = 0.914$ from ref. [10] with ε, v, E_{ac} and B as unknown parameters in the calculations, a similarly good fit to the μ_H versus T curve, with one set of best-fit parameters, could be obtained. The final values of the parameters, with their corresponding standard deviations of the fitted points, thus obtained together with those used in the analysis are listed in Table 1, and the resulting fitted curve is shown in Fig. 3. It is to be noticed that the estimated value of $v = 1.9 \times 10^5$ cm/s is similar to those found for most of the I–III–VI_2 tetragonal chalcopyrite compounds [8, 9]. Also, the value of $E_{ac} = 16.0$ eV/unit dilation is in the range of the values obtained from measurements of the fundamental optical energy gap E_g versus temperature T, E_g versus pressure as well as from mobility data, for the I–III–VI_2 [8, 16, 17, 18] and II–IV–V_2 [19] tetragonal chalcopyrite compounds and alloys.

4. Conclusions

From the analysis of the resistivity and the hole concentration versus T data the presence of an acceptor level located at about (43.4 $\pm$ 1.4) meV above the valence band is detected. At the present time, the origin of this level is unknown. In order to study the origin of this level, single crystal samples of this compound are being grown by the Bridgman method. Then, the electrical measurements will be carried out on the as-grown samples as well as on samples annealed both in vacuum and in the presence of elemental Cu, Fe, Ge or Se.

The results showed that a good fit of the μ_H against T data can be obtained using the scattering of charge carriers by ionized impurities, the combined acoustic and nonpolar optical modes as well as the space-charge effects. It is to be pointed out that the contribution due to neutral impurities was not needed in the analysis. As indicated above, the obtained values of m_p, v and E_{ac} are found to lie in the range of the reported values for the I–III–VI_2 and II–IV–V_2 tetragonal chalcopyrite materials.

Acknowledgements This work was financial supported by CONICIT-BID under grant NM-09 and CDCHT of the Universidad de Los Andes. The authors are grateful to Dr. B. Fernandez, head of the Low-Temperature Division of U.L.A., for allowing the use of the electrical equipment.

References

[1] Y. Shapira, E. J. McNiff, Jr., N. F. Oliveira, Jr., E. D. Honig, K. Dwight, and A. Wold, Phys. Rev. B **37**, 411 (1988).
[2] G. H. McCabe, T. Fries, M. T. Liu, Y. Shapira, L. R. Ram-Mohan, R. Kershaw, A. Wold, C. Fau, M. Averous, and E. J. McNiff, Jr., Phys. Rev. B **56**, 6673 (1997).
[3] J. K. Furdyna and J. Kossut, Diluted Magnetic Semiconductors, Semiconductors and Semimetals, Vol. 25, Chap. 1., Eds. R. K. Willardson and A. C. Beer, Academic Press, New York 1988.
[4] P. A. Wolff, D. Heimann, E. D. Isaac, P. Becla, S. Foner, I. R. Ram-Mohan, D. H. Ridgley, K. Dwight, and D. Wold, High Magnetic Fields in Semiconductors Physics, Ed. G. de Landwehr, Springer-Verlag, Berlin 1988.
[5] R. Nitsche, D. F. Sargent, and P. Wild, J. Cryst. Growth **1**, 52 (1967).
[6] M. Quintero, R. Tovar, A. Barreto, E. Quintero, A. Rivero, J. Gonzalez, G. Sánchez Porras, J. Ruiz, P. Bocaranda, J. M. Brotto, H. Rakoto, and R. Barbaste, phys. stat. sol. (b) **209**, 135 (1998).
[7] J. S. Blakemore, Solid State Physics, Saunder, Toronto 1974.
[8] M. Quintero, C. Rincon, R. Tovar, and J. C. Woolley, J. Phys.: Condensed Matter **4**, 281 (1992).
[9] H. Neumann, D. Peters, B. Schumann, and G. Kün, phys. stat. sol. (a) **52**, 559 (1979).
[10] J. D. Wiley and M. DiDomenico, Jr., Phys. Rev. B **2**, 427 (1970).
[11] H. Brooks, Adv. Electron Phys. **7**, 85 (1955).
[12] E. H. Putley, The Hall Effect and Semiconductor Physics, Butterworth, London 1960.
[13] J. S. Blakemore, Semiconductor Statistics, Pergamon Press, New York 1962.
[14] Numerical Recipes: The Art of Scientific Computing, Cambridge University Press, 1987 (p. 523).
[15] L. R. Weisberg, J. Appl. Phys. **33**, 1817 (1962).
[16] M. Quintero, J. Gonzalez, and J. C. Woolley, J. Appl. Phys. **70**, 1451 (1991).
[17] J. Gonzalez, E. Calderon and F. Capet, phys. stat. sol. (b) **187**, 149 (1995).
[18] L.I. Haworth, I. S. Al-Saffar, and R. D. Tomlinson, phys. stat. sol. (a) **99**, 603 (1987).
[19] J. Gonzalez and Ch. Power, Crystal Res. Technol., **31S**, 21 (1996).